



HAL
open science

Hydrodynamic effect on biofouling of milli-labyrinth channel and bacterial communities in drip irrigation systems fed with reclaimed wastewater

Kevin Lequette, Nassim Ait-Mouheb, Nathalie Wéry

► **To cite this version:**

Kevin Lequette, Nassim Ait-Mouheb, Nathalie Wéry. Hydrodynamic effect on biofouling of milli-labyrinth channel and bacterial communities in drip irrigation systems fed with reclaimed wastewater. *Science of the Total Environment*, 2020, 738, pp.139778. 10.1016/j.scitotenv.2020.139778. hal-02859809

HAL Id: hal-02859809

<https://hal.inrae.fr/hal-02859809>

Submitted on 15 Jun 2022

HAL is a multi-disciplinary open access archive for the deposit and dissemination of scientific research documents, whether they are published or not. The documents may come from teaching and research institutions in France or abroad, or from public or private research centers.

L'archive ouverte pluridisciplinaire **HAL**, est destinée au dépôt et à la diffusion de documents scientifiques de niveau recherche, publiés ou non, émanant des établissements d'enseignement et de recherche français ou étrangers, des laboratoires publics ou privés.



Distributed under a Creative Commons Attribution - NonCommercial 4.0 International License

1 **Hydrodynamic effect on biofouling of milli-labyrinth channel and bacterial**
2 **communities in drip irrigation systems fed with reclaimed wastewater.**

3 Kévin Lequette^{1,2}, Nassim Ait-Mouheb² and Nathalie Wéry¹

4 ¹*INRAE, University of Montpellier, LBE, 102, Avenue des Etangs, 11100 Narbonne, France;*

5 ²*INRAE, University of Montpellier, UMR G-Eau Avenue Jean-François Breton, 34000*
6 *Montpellier, France*

7 Correspondence: kevin.lequette@gmail.com

8 Tel.: +33 (0)4 68 42 51 82

9

1 **Abstract**

2 The clogging of drippers due to the development of biofilms reduces the benefits and
3 is an obstacle to the implementation of drip irrigation technology in a reclaimed water
4 context. The narrow section and labyrinth geometry of the dripper channel results the
5 development of a heterogeneous flow behaviours with the vortex zones which it enhance the
6 fouling mechanisms. The objective of this study was to analyse the influence of the three
7 dripper types, defined by their geometric and hydraulic parameters, fed with reclaimed
8 wastewater, on the biofouling kinetics and the bacterial communities. Using optical coherence
9 tomography, we demonstrated that the inlet of the drippers (mainly the first baffle) and vortex
10 zones are the most sensitive area for biofouling. Drippers with the lowest Reynolds number
11 and average cross-section velocity v (1 l.h^{-1}) were the most sensible to biofouling, even if
12 detachment events seemed more frequent in this dripper type. Therefore, dripper flow path
13 with larger v should be consider to improve the anti-clogging performance. In addition, the
14 dripper type and the geometry of the flow path influenced the structure of the bacterial
15 communities from dripper biofilms. Relative abundancy of filamentous bacteria belonging to
16 Chloroflexi phylum was higher in 1 l.h^{-1} drippers, which presented a higher level of
17 biofouling. However, further research on the role of this phylum in dripper biofouling is
18 required.

19 **Keywords:** Drip irrigation; biofilm; flow behaviours; Optical Coherence Tomography;
20 High-throughput DNA sequencing

21 **1. Introduction**

22 The scarcity of water resources is driving the development of water-saving irrigation
23 techniques that enable integrated management of water resources. The reuse of reclaimed

24 wastewater (RWW) is an appropriate way to alleviate the problem of scarce water resources
25 especially in arid and semi-arid regions (Worako, 2015). Using RWW has several advantages
26 including reducing pressure on freshwater resources and on the need for nutrients (e.g.
27 nitrogen, phosphorus) for plant growth (Lazarova and Bahri, 2005) and can improve crop
28 yields (Wang et al., 2013). Drip irrigation is the most water efficient (up to >90%) and safest
29 technique for irrigation using RWW (Lamm et al., 2007). Drippers are usually composed of a
30 labyrinth-channel and an outlet basin compartment. The geometry of the channel promotes
31 the dissipation of the turbulent kinetic energy due to the zigzag flow path and allows water to
32 be delivered in drip form in an optimum quantity for crop growth. However, the labyrinth
33 channel is narrow (cross-section of around 1 mm) (Zhang et al., 2010) and thus sensitive to
34 clogging (Liu and Huang, 2009; Niu et al., 2013) which reduces drip irrigation advantages by
35 reducing irrigation uniformity (Dosoretz et al., 2010) and by increasing maintenance (e.g.
36 cleaning, replacing irrigation lines).

37 The process leading to clogging of the drippers is complex and the phenomenon is
38 influenced by several parameters including water quality (concentration of suspended solids
39 and chemical composition) (Lamm et al., 2007; Oliveira et al., 2017), the geometry of the
40 dripper (Li et al., 2019; Wei, 2011) as well as biological processes (Katz et al., 2014), the
41 latter are the most difficult to control when RWW is used (Lamm et al., 2007). Moreover,
42 biofilms in distribution networks can harbour contaminants and may impact the quality of the
43 water released to agroecosystems (Jjemba et al., 2010). Therefore, identifying and
44 understanding the mechanisms leading to biofilm development is necessary to optimize
45 control strategies. Previous studies have shown that flow velocity has an impact on the growth
46 of biofilm in both drip-irrigation pipes (Li et al., 2012; Mahfoud et al., 2009) and in drippers
47 (Gamri et al., 2014).

48 Previous studies have been carried out on the effect of hydrodynamics on the
49 development of biofilm in straight pipe systems. Thus, an increase in flow rate or shear stress
50 tends to promote the development of a thin and dense biofilm in the pipe wall (Lehtola et al.,
51 2006; Percival et al., 1999). However, the flow behaviour in a dripper is more complex and
52 heterogeneous than in pipes, where the flow is simplified, due to the narrow labyrinth flow
53 path. This milli-labyrinth channel induces non-isotropic conditions by the development of
54 turbulent regime with a main high velocity flow and vortex zones in the channel corners (Al-
55 Muhammad et al., 2019, 2016; Wei et al., 2012; Zhang et al., 2007). Qian et al., (2017)
56 studied the development of fouling in a milli-fluidic system fed with reclaimed wastewater
57 using the Optical coherence tomography (OCT). OCT method allows to monitor biofilm
58 formation non-invasively at a mesoscale (μm to mm range) and without staining (Derlon et
59 al., 2012; Dreszer et al., 2014; Qian et al., 2017; Wagner et al., 2010; West et al., 2016). They
60 reported that fouling occurs mainly in inlet channel regions and in low velocity vortices areas
61 as found by Ait-Mouheb et al., (2018).

62 Flow behaviour not only influences the development of biofilms but also the microbial
63 composition of the biofilms. Previous research on biofilms has shown that hydrodynamic
64 conditions can drive the microbial community of the biofilms (Besemer, 2015; Hou et al.,
65 2020; Rickard et al., 2004). Rochex et al., (2008) shown that increased shear stress reduced
66 bacterial diversity and slow down biofilm maturation and tend to maintain a young biofilm in
67 a Taylor-Couette reactor. However, in the context of the use of RWW, few authors have
68 examined the influence of dripper parameters (i.e. flow rate, cross section, and geometry of
69 the milli-channel) on microbial composition. Previous studies have described the microbial
70 communities present in biofilms of different drippers by analysing phospholipid-derived fatty
71 acids (PLFAs) (Yan et al., 2010, 2009; Zhou et al., 2017) and indicated that dripper flow rate
72 influenced the PLFAs distribution. These authors showed that three to seven types of PLFAs

73 associated with Gram-negative bacteria were common in biofilms inside drippers, suggesting
74 a significant role for these bacteria in biofilm development. However, in order to develop
75 effective biofilm control strategies, deeper community characterization is required. Recent
76 study used high-throughput sequencing to describe the bacterial communities present in
77 dripper biofilms to improve knowledge on fouling and to identify the microorganisms
78 responsible for fouling (Xiao et al., 2020; Zhou et al., 2019).

79 The objectives of the present study were to determine the effect of 3 commercial
80 drippers with different discharges (1) on biofouling in the dripper channel and (2) on the
81 bacterial communities in biofilms formed in drip irrigation systems fed by RWW. A non-
82 destructive microscopic time-monitoring observation system was developed to study biofilms
83 in commercial drippers with different flow rates (1, 2 and 4 l.h⁻¹) and known cross-sections.
84 The combined use of the Optical Coherence Tomography method and high-throughput
85 sequencing made it possible to monitor the development of the biofilm under different
86 hydraulic conditions while assessing the impact of these conditions on microbial structure.

87

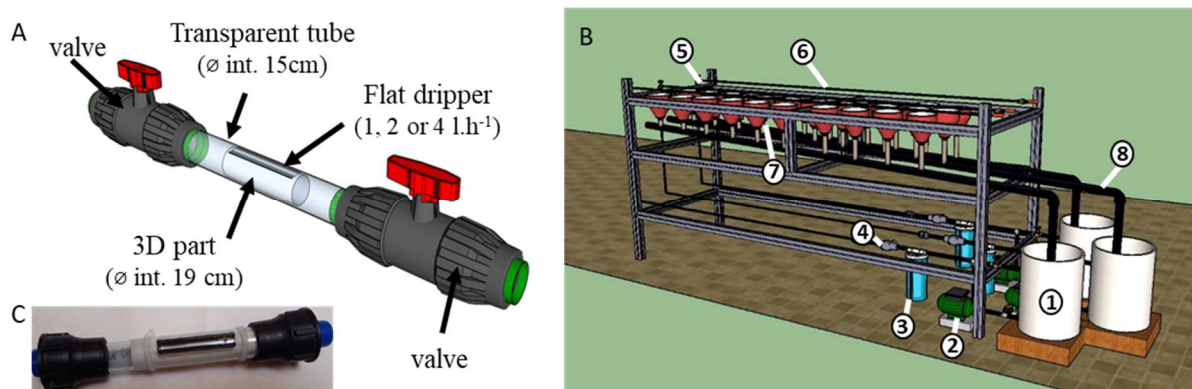
88 **2. Materials and Methods**

89 ***2.1. Experimental setup***

90 *2.1.1. Experimental setup and irrigation procedure*

91 The development of biofilm in drippers cannot be observed over time because drippers are
92 walled inside opaque irrigation pipes (black polyethylene tubes). Thus, commercial non-
93 pressure compensating drippers (NPC) (model D2000, Rivulis Irrigation SAS, Lespinasse,
94 France) with different flow path geometry and different flow rates (1, 2 and 4 l.h⁻¹) (Table 1)
95 were placed in a transparent tube (internal diameter 15mm, TubClair, Vitry-le-François,
96 France), allowing to see biofilm development along the channel over time. A solid tube with

97 an internal diameter of 19mm (ABS+, Stratasys U-print SE plus, Stratasys Ltd, Eden Prairie,
 98 Minnesota, US) pressed the dripper against the walls of the transparent tube (Figure 1.A,C).
 99 Finally, an outlet hole (internal diameter 2mm) was pierced in the transparent tube above the
 100 outlet basin. Nine drippers were connected to each other according with the type of dripper
 101 using polyethylene tubing (length 10cm, internal diameter 20mm) and valves (internal
 102 diameter 20mm) (total length 3m). Then, 3 lines were built (one per dripper type). The valves
 103 were used to keep the drippers under water when they were disconnected from the irrigation
 104 line for analysis. Each of the three lines was connected to a separate tank (total volume 60l)
 105 and a pump (JetInox 82M, DAB, Saint-Quentin-Fallavier, France) (Figure 1.B). A screen
 106 filter (mesh size 0.13mm) was installed to reduce the physical clogging of emitters following
 107 the technical recommendations of this type of dripper. The inlet pressure was set at 0.08 MPa
 108 with a pressure gauge. A gutter was installed below each lateral line to collect the water
 109 discharged from the drippers during the experiments. The gutters returned the discharged
 110 RWW to the respective tanks, enabling the recycling of water. The lines were supplied twice a
 111 day five days out of seven for 1h, with an interval of 6h off. The outlet flow rate from the
 112 drippers was measured weekly to evaluate emitter performance. Drippers are considered
 113 clogged when there is a decrease of at least 25% in the expected flow rate. The system was
 114 not flushed during the entire four-month experiment (from April to August 2018).



115

116 **Figure 1. Dripper system (A, C) and test bench (B). The drippers were placed in a**
 117 **transparent tube to enable optical measurements. The test bench was composed of 1. a**
 118 **tank (60l); 2. a water pump; 3. a 0.13mm mesh screen filter; 4. a pressure reducer; 5. a**

119 **pressure gauge; 6. the drip line with an emitter system located at 10-cm intervals; 7. a**
120 **collector; 8. a gutter.**

121

122 Table 1 lists the dripper characteristics (D1 to 3) commonly used in drip irrigation system.

123 The geometric parameters, including flow path length (L), width (W), depth (D) and cross-

124 sectional area (D_h) are specific to the dripper type, which influence the type of flow in the

125 dripper path. These parameters were further integrated as two dimensionless parameters,

126 including the width-depth ratio (W/D) and the relative radius ($A^{1/2}/L$), as proposed by Li et al.

127 (2019). Then, the hydraulic parameters, including the outflow (q), the Reynold number (Re)

128 and the inlet average cross-sectional velocity (v), are related to these geometric parameters.

129 In order to know the hydraulic conditions at the inlet channel, the flow regimes were

130 characterized by a Reynolds number (Re).

131 The Reynolds number (Re) was computed using the following formula:

132
$$Re = \frac{\rho v D_h}{\mu} \quad (\text{Equation 1})$$

133 where ρ is water density (kg.m^{-3}), v the water velocity across the pipe (m.s^{-1}), D_h the hydraulic

134 diameter (m), and μ the water viscosity (Pa s).

135 The Reynolds number of the studied drippers is between 305 and 926 at the inlet of labyrinth.

136 It should be noted that these Re correspond to laminar flow regime in the case of straight

137 pipes for example. However, due to the labyrinth geometry and small flow cross-sections, it is

138 assumed that flow behaviours in studied drippers correspond to turbulent regime (Li et al.,

139 2006; Zhang et al., 2016).

140 The hydrodynamic radius (or hydraulic diameter), D_h , was calculated for a rectangular cross-
141 section as:

142
$$D_h = \frac{4A}{P} \quad (\text{Equation 2})$$

143 where A: area (mm) and P for the perimeter (mm).




144

145

146

147
148
149
150
151

152 **Table 1. Dripper parameters**

Dripper	Structure of the dripper flow path	Geometric parameters of the path							Hydraulic parameters				
		L	W	D	D_h	Volume of the path (mm ³)	$\frac{W}{D}$	$\frac{D_h^{1/2}}{L}$	q (l.h ⁻¹)	Re	v (m.s ⁻¹)	$\cdot x$	CV (%)
D1		103.4	1.01	0.8	1.02	127	1.26	0.009	1	305	0.34	0.4	1.4
D2		94.1	1.03	0.9	1.12	142	1.14	0.011	2	579	0.60	0.4	1.9
D3		47.4	1.35	1.1	1.17	129	1.23	0.023	4	926	0.78	0.4	2.5

153 L : length of the flow path, W : width of the flow path, D : depth of the flow path, q : flow rate,
154 v : average cross-section velocity D_h : hydraulic diameter, $\cdot x$: pressure's exponent, CV:
155 Coefficient of variation

156 *2.1.2. Physical-chemical and microbiological quality of the RWW*

157 The irrigation lines were supplied with reclaimed wastewater from the Murviel-Les-
158 Montpellier in the South of France, (43.605034° N, 3.757292° E). The wastewater treatment
159 plant is designed around stabilisation ponds with three successive lagoons (13 680 m³, 4784
160 m³ and 2700 m³) and a nominal capacity of 1,500 Inhabitant Equivalent. The RWW was
161 placed in a 60l tank and changed twice a week to maintain the quality close to that of the
162 wastewater from the treatment plant. Each week (n=16), several physical-chemical and
163 microbiological analyses were performed to evaluate the RWW quality. Chemical oxygen
164 demand (COD), ammonia, nitrate, and phosphorus concentrations (mg l⁻¹) were measured
165 with a spectrophotometer (DR1900, Hach Company, Loveland, CO, USA) using Hach
166 reagents[®]. Conductivity and pH were measured with probes (TetraCon[®] 925 and pH-

167 Electrode Sentix® 940, WTW, Wilhelm, Germany). Faecal coliforms, *E. coli*, and *Enterococci*
 168 were quantified using the IDEXX method (Colilert18 and Enterolert, IDEXX Laboratories,
 169 Westbrook, ME) according to the supplier's recommendations. The main effluent properties
 170 are listed in Table 2.

171 **Table 2. Physico-chemical characteristics of the RWW**

Characteristics	Units	Mean (n=24)	SD
s- COD	mg l ⁻¹	70.3	7.6
Total suspended solids	mg l ⁻¹	61	24.2
Ammonia	mg l ⁻¹	25.7	7.8
Nitrate	mg l ⁻¹	0.7	0.1
Phosphorus	mg l ⁻¹	4.9	0.9
Conductivity	μS cm ⁻¹	1101.4	51.5
Dissolved oxygen	mg l ⁻¹	6.8	1.5
pH		6.9	0.8
Total coliforms	MPN/100ml	6.1x10 ⁵	6.4x10 ⁵
<i>Escherichia coli</i>	MPN/100ml	5.9x10 ⁴	5.1x10 ⁴
<i>Enterococci</i>	MPN/100ml	3.2x10 ⁴	4.6x10 ⁴

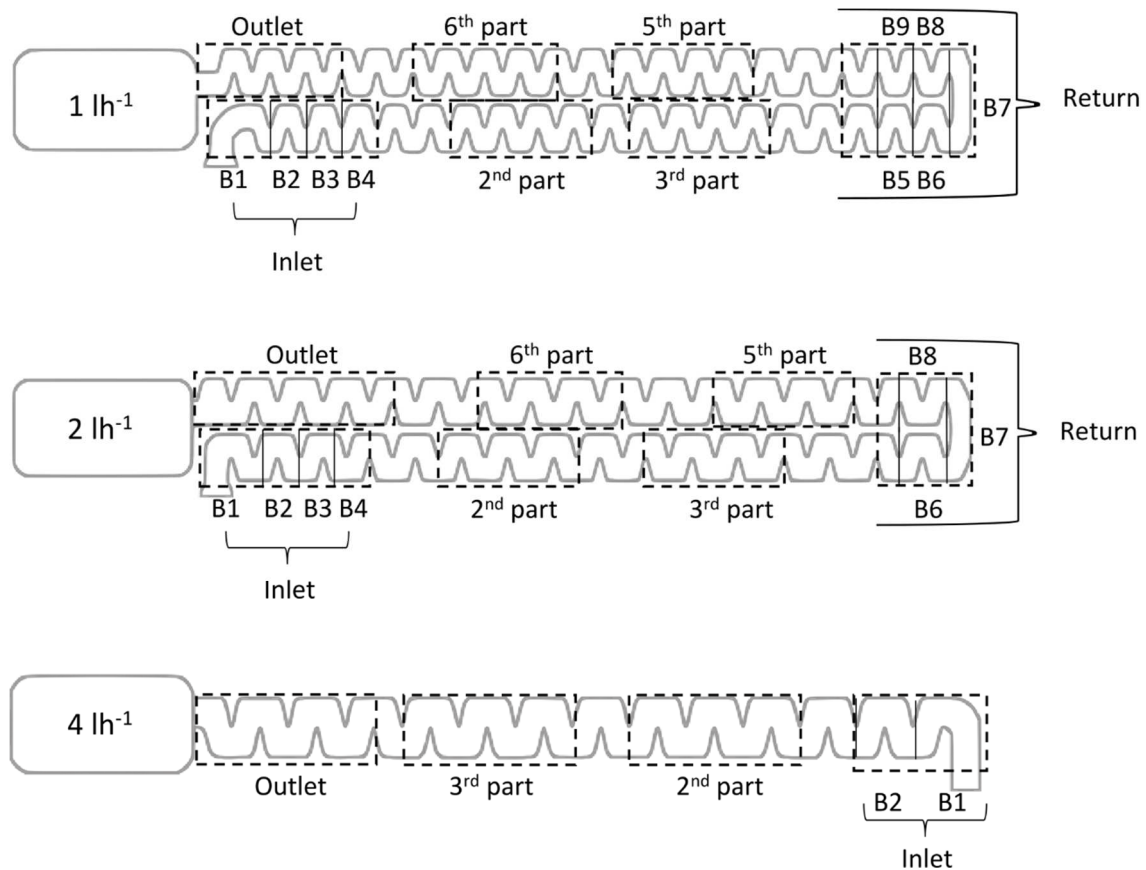
172

173 2.2. Image acquisition and processing

174 2.2.1. Image acquisition

175 Optical coherence tomography (OCT) was used to study the biofilm kinetics in
 176 drippers and along the milli-channel throughout the experimental period. The measurements
 177 were performed in situ and non-invasively through the transparent tube. For the
 178 measurements, the valves of the dripper systems were closed to keep the drippers in water,
 179 and then the dripper in its tubing was disconnected from the irrigation line. Measurements
 180 were taken at least once every two weeks and each time all drippers were analysed. After the
 181 OCT measurement, each dripper was replaced on the test bench at its initial location. Three-
 182 dimensional OCT measurements were acquired using a Thorlabs GANYMEDE II OCT
 183 (LSM03 lens, lateral resolution: 8μm; Thorlabs GmbH, Lübeck, Germany). The axial voxel

184 size in water ($n = 1.333$) of GANYMEDE II is $2.1 \mu\text{m}$. OCTs have a centre wavelength of
 185 930 nm . Due to the length of the drippers, the labyrinth channel was divided into eight parts
 186 (inlet, part 2, part 3, return, part 6, part 7, and end; Table S1 in Supplementary material) to
 187 study biofouling in different parts of the channels (Figure 2).
 188



189
 190 **Figure 2. Schematic diagram of the geometric channel from the drippers. The dotted**
 191 **boxes correspond to the study areas. The length and width (in mm) of each baffle are**
 192 **listed in the Table S1 in Supplementary material.**

193

194 2.2.2. Image processing

195 First, 3-D OCT datasets were processed in Fiji (running on ImageJ version 1.50b,
 196 Schindelin et al., (2009)) and converted into 8-bit grayscales. The datasets were resliced from
 197 top to bottom into image stacks and regions of interest (inlet and return areas) were selected.
 198 The remaining parts were allocated to the background (black). Secondly, an in-house code

199 was used to detect the pixels associated with the plastic tube and removed using MATLAB
200 R2018r (MathWorks®, version 2018b). A threshold (adapted to each dataset) was applied to
201 binarize the dataset and the region above the interface was quantified as biofilm. For each
202 position (x, y), the pixels associated with the biofilm (up to the threshold) were summed (on
203 z) to obtain the thickness of the biofilm. The volume of the baffles differed with the dripper
204 (e.g. 4.7, 5.8 and 10.7 mm³ for B1 and 3, 5 and 8.5 mm³ for B2 for 1, 2 and 4 l.h⁻¹
205 respectively, Figure 2). Therefore, to compare the level of fouling between drippers, the
206 biofouling volume was normalized by the volume of the corresponding baffle. The volumetric
207 coverage of the biofilm (%) was calculated for each baffle according to Equation 3:

$$208 \quad \text{Volumetric Coverage \%} = \frac{V_{\text{biofilm}}}{V_{\text{baffle}}} \times 100 \quad (\text{Equation 3})$$

209 where V_{biofilm} is the biofilm volume and V_{baffle} is the volume of the baffle.

210 **2.3. Analysis of the microbial communities**

211 *2.3.1. Sampling the biofilm and reclaimed wastewater*

212 Three drippers in each line were chosen at 32, 72 and 115 days and replaced by new
213 ones to ensure the functioning of the system. However, these new drippers have not been
214 analyzed. Each dripper in the transparent tube was extracted with sterile clamps and placed
215 directly in a sterile tube and stored at -20°C until DNA extraction. RWW was filtered (15 to
216 30 mL) each week through 0.2 µm (Supor® 200 PES Membrane Disc Filter, Pall
217 Corporation) to analyse the bacterial community in the reclaimed wastewater. Filters were
218 stored at -20°C until DNA extraction.

219 *2.3.2. DNA extraction*

220 DNA was extracted using the PowerWater® DNA Isolation Kit (Qiagen, Hilden, Germany).
221 Samples (drippers or filters) were placed in 5 mL tubes containing beads. The manufacturer's

222 instructions were then followed. The DNA concentration was measured, and purity checked
223 by spectrophotometry (Infinite NanoQuant M200, Tecan, Austria). Extracted DNA was stored
224 at -20°C.

225 2.3.3. *Bacterial quantification by qPCR*

226 Total bacterial quantification was performed by qPCR on biofilms from drippers targeting the
227 V9 region from 16S rDNA. The amplification reactions were performed in triplicate, and at
228 two dilutions to check for the absence of inhibition of the PCR reaction. Reaction mixes
229 (12µl) contained 2.5µl of water, 6.5µl of Super Mix qPCR (Invitrogen), 100nM forward
230 primer BAC338 (5'-ACTCCTACGGGAGGCAG-3'), 250nM of reverse primer BAC805 (5'-
231 GACTACCAGGGTATCTAAT CC-3') and 50nM of probe BAC516 (Yakima Yellow-
232 TGCCA GCAGC CGCGG TAATA C -TAMRA) (Yu et al., 2005). The cycling parameters
233 were 2 min at 95°C for pre-incubation of the DNA template, followed by 40 cycles at 95°C
234 for 15 sec for denaturation and 60°C for 60 sec for annealing and amplification.

235 2.3.4. *Illumina sequencing*

236 PCR amplified the V4-V5 region of 16S rRNA genes with 30 cycles (annealing temperature
237 65°C) using the primers 515U (5'-GTGYCAGCMGCCGCGGTA-3') and 928U (5'-
238 CCCCgycaattcmtttragt-3') (Wang and Qian, 2009). Adapters were added for
239 multiplexing samples during the second amplification step of the sequencing. The resulting
240 products were purified and loaded onto the Illumina MiSeq cartridge for sequencing of paired
241 300 bp reads according to the manufacturer's instructions (v3 chemistry). Sequencing and
242 library preparation was performed at the Genotoul Lifescience Network Genome and
243 Transcriptome Core Facility in Toulouse, France (get.genotoul.fr). Mothur (version 1.39.5)
244 (Schloss et al., 2009) was used to associate forward and reverse sequences and clustering at
245 four different nucleotides over the length of the amplicon. Uchime (Edgar et al., 2011) was

246 used to identify and remove chimera. Sequences that appeared less than three times in the
247 entire data set were removed. In all, 16S rRNA sequences were aligned using SILVA SSURef
248 NR99 version 128 (Schloss et al., 2009). Finally, sequences with 97% similarity were sorted
249 into operational taxonomic units (OTUs) (Nguyen et al., 2016). The chloroplast sequences
250 were removed from the raw data. Finally, BLAST (<http://www.ncbi.nlm.nih.gov/BLAST/>)
251 was used to locate publicly available sequences closely related to the sequences obtained from
252 the samples. A total of 11,357,162 reads were grouped in 7730 OTUs at the 97% similarity
253 level. The rarefaction curves indicated that the sequencing depths of all samples were
254 adequate (Figure S4 in Supplementary material).

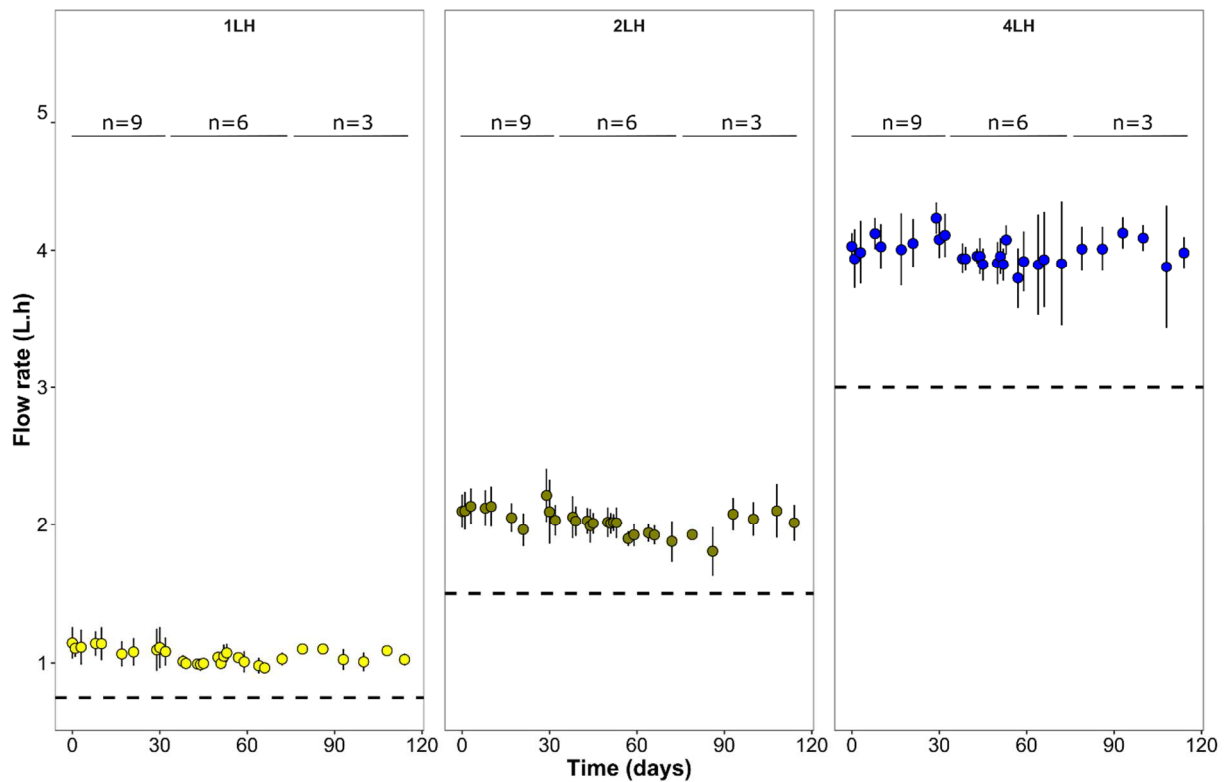
255 *2.4. Statistical analyses*

256 The effect of the different commercial types of drippers (with specific geometry and hydraulic
257 parameters) on the kinetics and bacterial composition of the biofouling was evaluated. The
258 kinetics of biofilm development were evaluated by modelling the biofilm formation rate using
259 linear and spline models. The sequencing data were processed under R v3.4 ([www.r-](http://www.r-project.org)
260 [project.org](http://www.r-project.org)) using the R-Studio (<http://www.rstudio.com/>) phyloseq package (McMurdie and
261 Holmes, 2012). Kruskal-Wallis tests were performed to compare diversity and richness
262 indices over time and between the dripper types. For the comparison of bacterial community
263 structure, a dissimilarity matrix (Bray-Curtis) was performed and visualised using principal
264 coordinate analysis (PCoA). A one-way analysis of similarities (ANOSIM) was used to
265 identify significant differences in community assemblage structure between samples based on
266 the origin of the sample (Clarke, 1993). The OTUs that contributed most to the divergence
267 between two types of dripper were identified using Similarity Percentage (SIMPER) analysis
268 (Clarke, 1993).

269 **3. Results**

270 **3.1. Areas favourable for the development of biofilm**

271 The optical methods and discharge measurements are performed in order to analyse the effect
272 of flow topologies along the three dripper channels. During the four month experiment,
273 dripper outflows was higher than 75% of expected flow rate and the drippers never became
274 clogged (Figure 3).

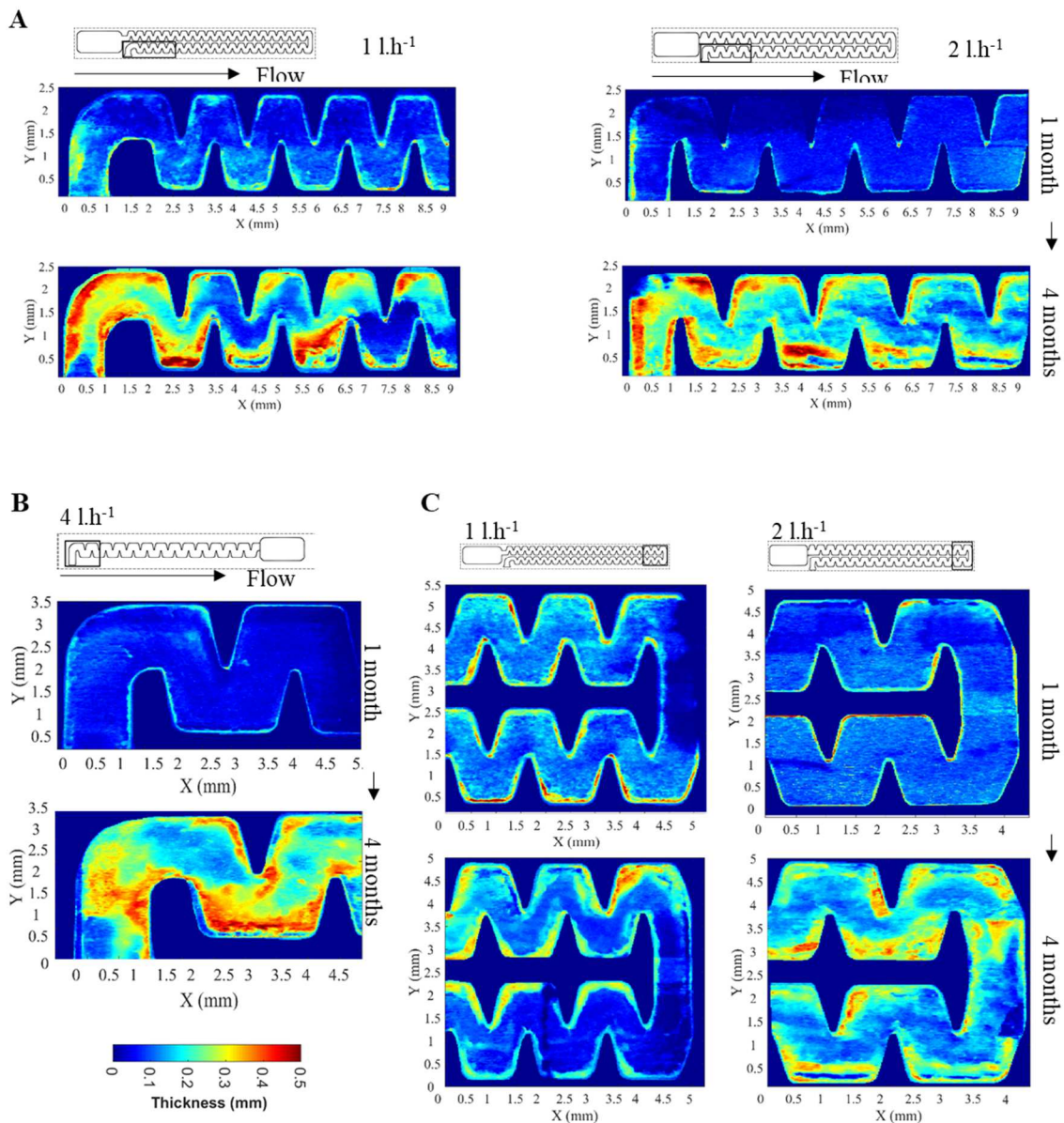


275

276 **Figure 3 Mean flow rate (and standard error) according to the dripper type.** The dotted
277 line of discharge of less than 75% corresponds to the limit usually set up to consider that a
278 dripper is clogged. n refers to the number of dripper of the lines.

279 In the first two weeks, the thickness of the biofilm was too low to be measured and the first
280 measurements were made after one month. Based on OCT analysis (Figure S1, S2 and S3 in
281 Supplemental material), the biofouling volume after 4 months tended to be higher at the inlet
282 areas (2.45, 3.32 and 2.19 mm³ for 1, 2 and 4 l.h⁻¹ drippers respectively) and decreased after
283 until the return area (with 1.62 and 2 mm³ of biofilm respectively, there is no return area in 4
284 l.h⁻¹). This means that inlet and return were the most sensible areas for clogging. Figure 4

285 shows the increase in biofouling thickness in the inlet and return dripper areas at one and four
 286 months. Over time, biological fouling at the inlet area increased, mainly in the first baffle and
 287 in corners, and gradually spread to the following corner baffles. After 4 months, the biofilm
 288 thickness was higher in the baffle corners for all the drippers, up to 0.5 mm while the
 289 thickness at the center of the channel was < 0.3 mm. The biofilm thickness in the return area
 290 increased mainly after the large bend (B7) in both types of drippers (Figure 4C).



291
 292 **Figure 4. Biofilm thickness measured using OCT method at the inlet of 1, 2 l.h⁻¹ drippers**
 293 **(A) and 4 l.h⁻¹ dripper (B) and in the return areas of drippers (C) measured after 1 and**
 294 **4 months.**

295 The volume of the baffles differed with the dripper. Therefore, to compare the level of
296 fouling between drippers, the biofouling volume was normalized by the volume of the
297 corresponding baffle (Equation 3). Mean biofouling of the inlet baffles increased over time in
298 all three types of drippers (Figure S5 in Supplemental material). The level of biofouling were
299 significantly influenced by the type of dripper ($\text{Chi}^2=115$, $p\text{-value} < 0.05$) and the time
300 ($\text{Chi}^2=54$, $p\text{-value} < 0.05$) and increased more rapidly in 1 and 2 l.h^{-1} drippers than in 4 l.h^{-1}
301 dripper types (Wald test, $p\text{-value} < 0.05$). After 4 months, the mean biofouling level at the
302 inlet were higher in the 1 l.h^{-1} (18%) and in 2 l.h^{-1} (15.9%) than in the 4 l.h^{-1} (11.8%) drippers
303 (conover test, $p\text{-value} < 0.05$). Therefore, the 1 l.h^{-1} dripper with lowest average cross-section
304 velocity (v), Reynolds number and the ratio W/D and $D_h^{1/2}/L$ were the most sensitive to
305 clogging.

306 Although the biofouling level of the first baffle tended to be higher, there was no
307 statistical effect of baffles on volumetric coverage over time. However, the volume of
308 biofouling in the first baffle was significantly higher in 1 l.h^{-1} drippers than in 2 l.h^{-1} and 4 l.h^{-1}
309 l.h^{-1} dripper types after four months with a mean volumetric coverage of 22.6%, 15.8% and 14.1
310 % for 1 l.h^{-1} , 2 l.h^{-1} and 4 l.h^{-1} drippers, respectively (Kruskal test, $p\text{-value} < 0.05$).

311 The mean increase in biofouling in the 1 l.h^{-1} drippers presented a sinusoidal dynamic
312 with up and down phases at the inlet baffle (Figure S5 in Supplemental material). This could
313 mean several detachment events occurred. The same cycle was observed in the 2 and 4 l.h^{-1}
314 dripper types but only in the first baffle. The detachment event occurred at ~ 3 months in the 4
315 l.h^{-1} drippers whereas the first event appeared at 1 month in the 2 l.h^{-1} dripper types. After this
316 baffle, the increase in biofouling was linear. At the return zone in 1 and 2 l.h^{-1} drippers, the
317 volumetric coverage increased over time but was heterogeneous. Thus it was not possible to
318 define kinetic models.

319 The type of dripper (flow rate and flow cross-section) influenced the level of fouling
 320 of the labyrinth with a higher fouling rate in 1 l.h⁻¹ drippers (narrower flow cross-section and
 321 lower average cross-section velocity).

322 **3.2. Microbial diversity differed between dripper biofilms and reclaimed**
 323 **wastewater**

324 The structure of the bacterial communities in biofilms collected in the three types of drippers
 325 were compared using 16S rDNA Illumina sequencing. The bacterial communities in the
 326 biofilms were also compared with the communities present in reclaimed wastewater. The
 327 chloroplast sequences were removed from the raw data and represented 1.6% and 5.4% of the
 328 total sequences in biofilms and in RWW samples, respectively. Microscopic observations of
 329 the biofilms in the pipes (data not shown) also revealed the presence of eukaryotic
 330 microorganisms (bacterial predators) but the biofilms were still mainly composed of bacteria.

331 Mean DNA concentration increased significantly between the sampling events for
 332 each dripper types drippers (Table 3, p<0.05) but there were no differences between the
 333 dripper types (p>0.05). On the other hand, the number of bacteria remained unchanged over
 334 time and were similar between the drippers (Table 3, p>0.05), meaning that the increasing of
 335 the DNA concentration was probably due to other types of organisms that we observed in
 336 pipe biofilms in previous experiments (i.e. eukaryote, algae).

337

338 **Table 3. DNA concentration and quantification of bacteria by qPCR in dripper biofilms**

Sampling time (days)	Dripper flow rate (l.h ⁻¹)	Mean DNA concentration (µg/µl)	Mean of bacteria /dripper (16S copies/dripper)
32	1	137.4±67.9 ^a	6.2±0.9 x 10 ^{9a}
	2	113.9±42.7 ^a	5.7±0.6 x 10 ^{9a}
	4	118.1±26.8 ^a	9.9±1.2 x 10 ^{9a}
72	1	220.4±34.6 ^a	9.2±0.5 x 10 ^{9a}
	2	287.4±113.8 ^a	1.2±0.05 x 10 ^{10a}
	4	194.4±20.2 ^a	4.3±2.3 x 10 ^{9a}

115	1	325.2±70.8 ^a	8.7±0.4 x 10 ^{9a}
	2	387.8±164.1 ^a	1.4±0.5 x 10 ^{10a}
	4	346.1±34.5 ^a	5.4±1.4 x 10 ^{9a}

339 Kruskal-test and Wilcoxon ad hoc tests were performed on each sampling event to compare
340 the values between the drippers (n= 3 for each type of dripper on each sampling event); letters
341 show Wilcoxon test results.
342

343 Although fouling levels were higher in the 1 l.h⁻¹ dripper type, the richness and
344 diversity indices of the biofilms did not differ significantly and increased similarly between
345 the dripper over time (p-value > 0.05) (Table 4) meaning that the arrival of new species in
346 biofilms could settled regardless of hydrodynamic conditions. The richness and diversity
347 indices of RWW were lower than those in the dripper biofilms. The majority of operational
348 taxonomic units (OTUs) were shared by all the biofilms (Figure S6 in Supplemental material).
349 Some OTUs and bacterial genera were specific to the dripper flow, but their relative
350 abundance was less than 0.1% (Table S2 and Figure S6 in Supplementary material).

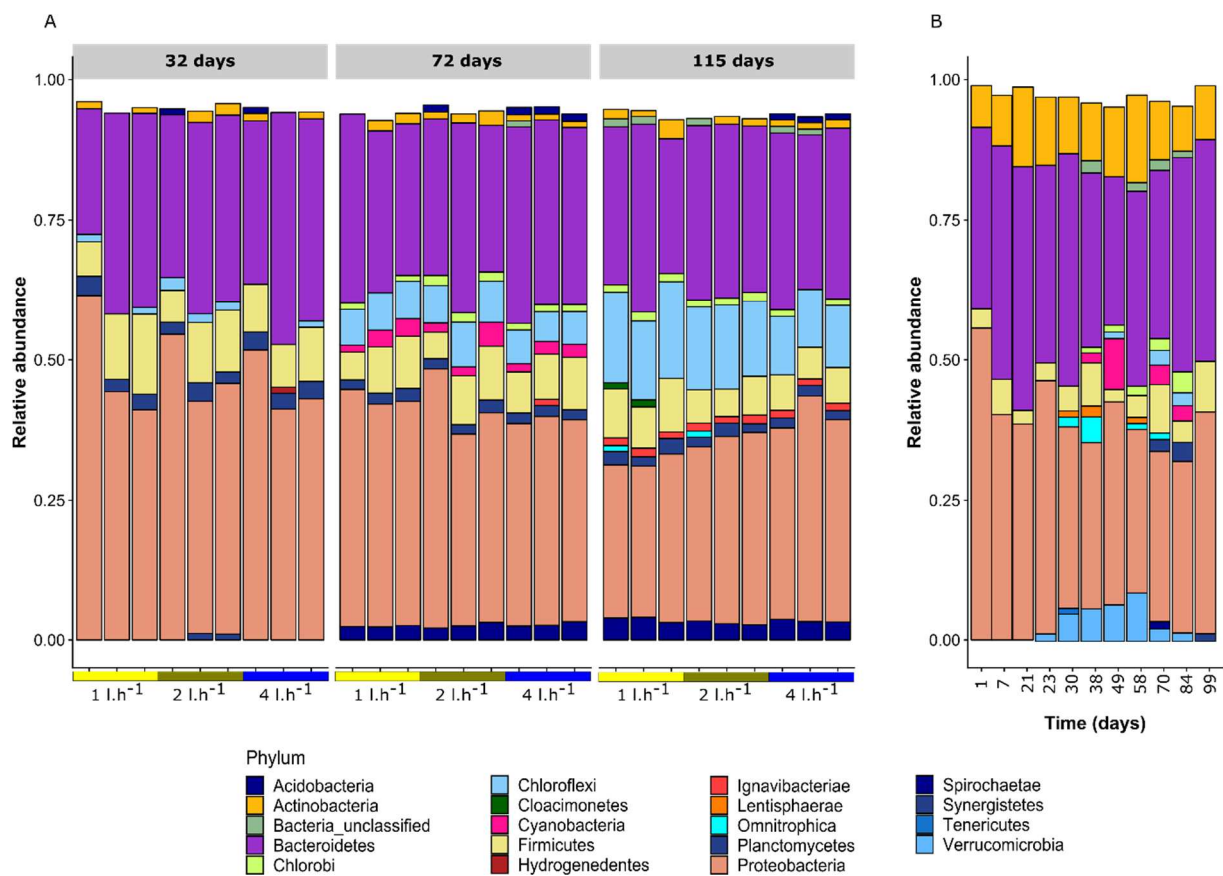
351 **Table 4. Estimated species richness and diversity indices according to the dripper flow**
352 **rate and the RWW**

Samples	Flow rate (l.h ⁻¹)	Age (Days)	Richness indices		Diversity indices	
			Observed	Chao1	Shannon	1/Simpson
Dripper	1 (n=3)	32	786 ± 36 ^a	786 ± 36 ^a	4.7 ± 0.1 ^a	40 ± 7 ^a
		72	1215 ± 18 ^b	1215 ± 18 ^b	5.5 ± 0.1 ^b	88.4 ± 15.8 ^b
		115	1640 ± 135 ^c	1640 ± 135 ^c	5.9 ± 0.1 ^c	149.5 ± 17.4 ^c
	2 (n=3)	32	752 ± 61 ^a	752 ± 61 ^a	4.7 ± 0.1 ^a	42.3 ± 2.7 ^a
		72	1286 ± 188 ^b	1286 ± 188 ^b	5.5 ± 0 ^b	90.3 ± 6.6 ^b
		115	1758 ± 92 ^c	1758 ± 92 ^c	5.8 ± 0.1 ^c	114.2 ± 9.4 ^c
	4 (n=3)	32	783 ± 54 ^a	783 ± 54 ^a	4.6 ± 0.1 ^a	40.4 ± 7.7 ^a
		72	1360 ± 23 ^b	1360 ± 23 ^b	5.6 ± 0 ^b	106.7 ± 3.9 ^b
		115	1726 ± 30 ^c	1726 ± 30 ^c	5.8 ± 0 ^c	116.6 ± 3.3 ^c
RWW (n= 11)	-	836 ± 310	836 ± 310	4.2 ± 0.7	32.6 ± 22.9	

353 Kruskal test and the Wilcoxon ad hoc test were performed for each dripper (n= 3 at each
354 sampling); the letters show the results of the Wilcoxon test.

355 Proteobacteria, Bacteroidetes, Firmicutes and Chloroflexi were the main phyla in the
356 dripper biofilms (Figure 4A). The main phyla found in RWW were Proteobacteria (25-55%)

357 mainly composed of β -Proteobacteria (10-34%) and γ -Proteobacteria (2-34%), followed by
 358 Bacteroidetes (22-40%) and Actinobacteria (7-14%) (Figure 5B). These differences indicate
 359 that among bacteria in the reclaimed wastewater, bacteria able to attach to the surface of the
 360 dripper under the corresponding flow regime were selected, especially among Firmicutes and
 361 Chloroflexi (Figure 5). From 49 days onwards, cyanobacteria phylum appeared in reclaimed
 362 wastewater, explaining the increase in cyanobacteria in the drippers on the second sampling
 363 events (72 days). The same observation was made concerning Spirochaetae and Chlorobi
 364 phyla. Thus, RWW influenced the bacterial structure and composition of the dripper biofilms.
 365 The structure of the biofilms in the drippers evolved over time according to changes in the
 366 microbial diversity in the reclaimed wastewater, and with the selection of some adapted taxa
 367 able to adhere to the surfaces, such as filamentous Chloroflexi bacteria.



368

369 **Figure 5. Relative abundance of bacterial phyla (>1%) in dripper biofilms (A) and in**
 370 **reclaimed wastewater (B).** For each sampling event, 3 drippers per dripper type were
 371 sampled.

372

373 ***3.3. The dripper flow parameters influenced the composition of the bacterial***
374 ***communities***

375 The impact of the type of dripper, defined both by geometric and hydraulic
376 parameters, on the structure of bacterial communities was first investigated at the phyla and
377 family taxonomic levels. Proteobacteria phylum was the most abundant phylum in the
378 biofilms (Figure 5) and was mainly composed of α -Proteobacteria, β -Proteobacteria (mainly
379 composed of members of the Comamonadaceae family), γ -Proteobacteria and δ -
380 Proteobacteria. At 32 days, the mean abundance of Proteobacteria was similar in all dripper
381 types, with 49, 47 and 45% in the 1, 2 and 4 l.h⁻¹ dripper biofilms, respectively (Kruskal-test,
382 p-value > 0.05). At 115 days, the mean relative abundance of Proteobacteria (and more
383 specifically β -Proteobacteria) was significantly lower in the 1 l.h⁻¹ dripper biofilms than in
384 the 2 and 4 l.h⁻¹ dripper biofilms (Kruskal-test, p-value < 0.05) and decreased significantly
385 until 28% versus 33 and 37% for the 2 and 4 l.h⁻¹ dripper biofilms, respectively.

386 The phylum of Bacteroidetes was mainly composed of Sphingobacteriia
387 (Chitinophagaceae, Lentimicrobiaceae, Saprospiraceae and Sphingobacteriaceae class
388 members), Bacteroidia (mainly Draconibacteriaceae and Rikenellaceae member families) and
389 Bacteroidetes_vadinHA17. There was no effect of the type of dripper on the mean relative
390 abundance of Bacteroidetes (~ 30% over time in each dripper type, Kruskal test, p-value >
391 0.05). Over time, the relative abundance of Sphingobacteriia and Bacteroidia decreased while
392 the relative abundance of Bacteroidetes_vadinHA17 increased in the three types of drippers.

393 The mean relative abundance of Chloroflexi (mainly composed of Anaerolineaceae
394 and Caldilineaceae member family) increased significantly over time and was significantly
395 higher in 1 l.h⁻¹ dripper biofilms after 115 days (16% versus 14% and 10% in 1, 2 and 4 l.h⁻¹
396 dripper biofilms, respectively, Kruskal test, p-value < 0.05). At 115 days, the mean relative

397 abundance of the Anaerolineaceae family was significantly higher in 1 l.h⁻¹ dripper biofilms
398 than in the 4 l.h⁻¹ dripper biofilms (Kruskal test, p-value < 0.05). There were no significant
399 differences in the Firmicutes phylum (mainly represented by Christensenellaceae,
400 Clostridiaceae and Ruminococcaceae), according to the dripper types or over time (Kruskal
401 test, p-value > 0.05).

402 The impact of flow rates on bacterial communities was then investigated at the genus level.
403 Table S3 lists the 10 top genera found in all the dripper biofilms over time. At 32 days, the 1
404 l.h⁻¹ dripper biofilms were dominated by the Comamonadaceae family (6%) including
405 *Hydrogenophaga* genus (9%) and *Pseudoxanthomonas* (3%). The mean relative abundance of
406 the *Hydrogenophaga* genus was significantly influenced by the flow rate (Kruskal test, p-
407 value < 0.05) and was higher in the 1 l.h⁻¹ dripper biofilms (3% and 4% for 2 and 4 l.h⁻¹
408 dripper biofilm, respectively). Over time, the mean relative abundance of members of the
409 Comamonadaceae family and of the *Hydrogenophaga* genus decreased significantly in the 1
410 l.h⁻¹ (Kruskal test, p-value < 0.05), close to the relative abundance in 2 and 4 l.h⁻¹ dripper
411 biofilms at the end (Kruskal test, p-value > 0.05). Although Proteobacteria phylum dominated
412 at 115 days, some members belonging to Bacteroidetes phylum increased over time as
413 Lentimicrobiaceae family and Bacteroidetes_vadinHA17 and dominated in all three drippers
414 at 115 days (Kruskal test, p-value > 0.05).

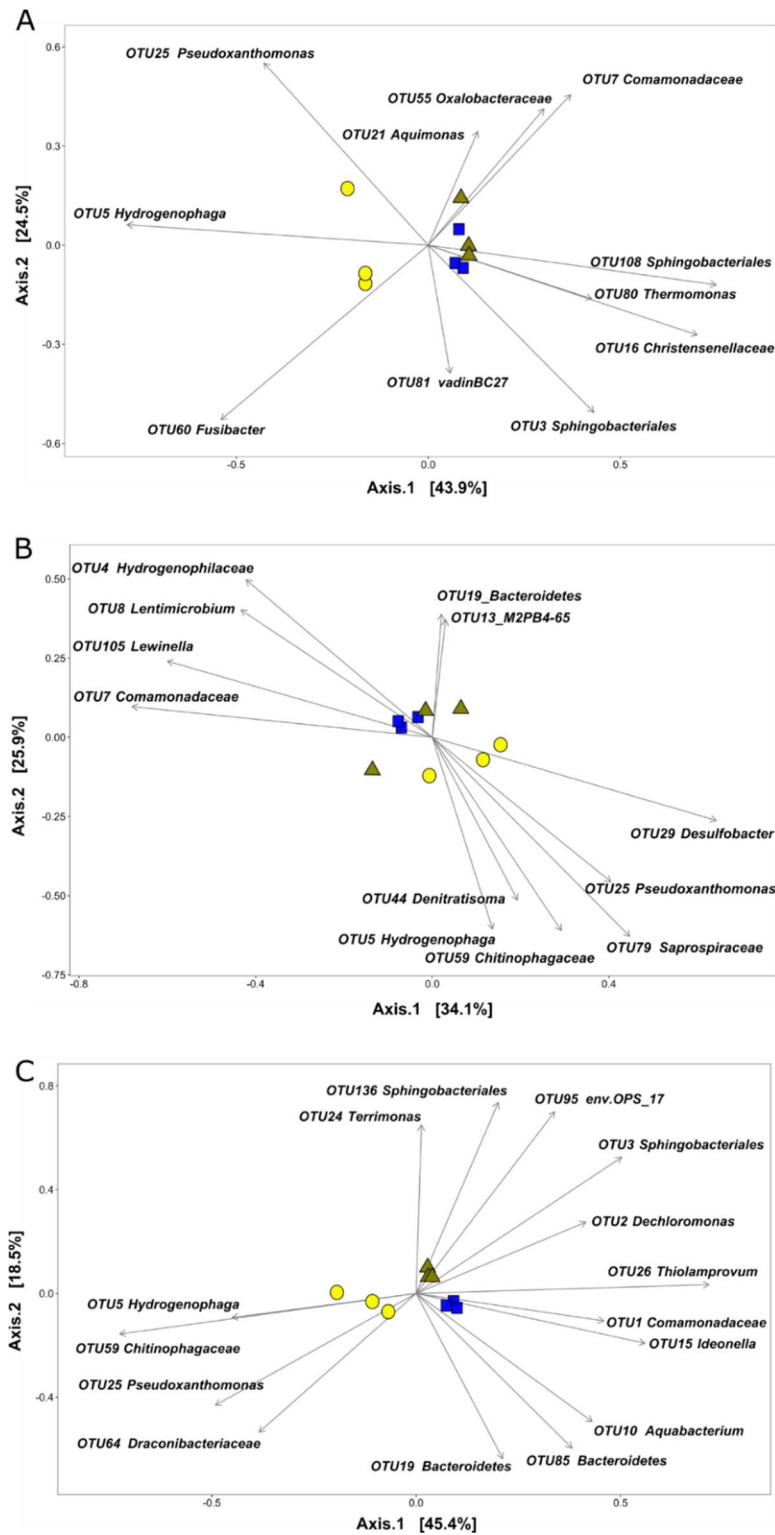
415 Even if the majority of the genera were the same in the different drippers and on the
416 sampling occasions, some genera with low abundance (<1%) depended specifically on the
417 dripper flow rate and the sampling time (Table S2, Figure S6 in Supplemental material). For
418 instance, only *Vulcaniibacterium* and *Microvirga* genera were found in the 1 l.h⁻¹ dripper at
419 32 and 72 days. This means that hydrodynamic conditions influenced both the dominant and
420 less abundant bacterial taxa.

3.4. *Dripper hydraulic properties impact bacterial community structure*

PCoA was performed to compare the structure of bacterial communities between the three types of dripper over time and confirmed that the bacterial community in the dripper biofilms changed depending on hydraulic dripper properties (Figure 6). At 32 days, the bacterial populations in 2 and 4 l.h⁻¹ were clustered (one-way ANOSIM, R=0.71, p < 0.05). The bacterial communities in the 1 l.h⁻¹ dripper biofilms formed a second cluster (Figure 6, A). This means that the hydraulic conditions had little influence on the structure of the microbial community in 2 and 4 l.h⁻¹ compared to that in the 1 l.h⁻¹ dripper biofilms at the first stage of development. At the end of the experiment (Figure 6, C) the bacterial community in 2 and 4 l.h⁻¹ diverged and formed specific groups (one-way ANOSIM, R=0.65, p<0.05).

The main contributors of the bacterial community were identified using SIMPER analyses and were shown to change over time. Those explaining 50% of the global bacterial divergence are indicated in Figure 5. At 32 days, 11 OTUs played a significant role in bacterial community divergence. *Pseudoxanthomonas* (OTU 25), *Hydrogenophaga* (OTU 5) and *Fusibacter* genera (OTU 60) were the main contributors and were associated with the 11.l.h⁻¹ drippers. These genera were also the main genera found in 1 l.h⁻¹ dripper biofilms at 32 days (Table S3 in Supplemental material). At 115 days, 15 OTUs significantly contributed to divergence. *Hydrogenophaga* (OTU 5) and *Pseudoxanthomonas* (OTU 25) were still strong contributors associated with 1 l.h⁻¹ dripper biofilms. *Aquabacterium* (OTU 10), *Ideonella* (OTU 15) and Bacteroidetes members (OTU 19, OTU 85) were associated with the 4l.h⁻¹ dripper biofilms, whereas Sphingobacteriales family members (OTU 3, OTU 136) and *Terrimonas* genus (OTU 24) were associated with 2l.h⁻¹ dripper biofilms.

443



444

445 **Figure 6.** PCoA ordination plot of bacterial communities found in 1 l.h⁻¹ (●), 2 l.h⁻¹ (▲)
 446 and 4 l.h⁻¹ (■) dripper biofilms at 32 days (A), 72 days (B) and 115 days (C). The analysis
 447 was based on Bray-Curtis similarity coefficients. Arrows indicate the orientation and
 448 contribution of the OTUs (most significant contributors explaining 50% of the global
 449 bacterial divergence).

450 **4. Discussion**

451 The main problem with the use of the drip irrigation supplied with reclaimed wastewater is
452 biofouling. Understanding the development of biofouling is the only way to limit the clogging
453 of drip irrigation systems. The labyrinth milli-channel drippers favour the formation of
454 heterogeneous flow with vortex zones. In this study, a laboratory experiment was performed
455 to investigate the kinetics of biofouling and changes in the bacterial communities over time as
456 a function of the hydrodynamic parameters (flow rate, cross-section) of the drippers. Three
457 types of commercial flat drippers used in agriculture with specific channel geometry and
458 different flow rates (1, 2 and 4 l.h⁻¹) were installed on a test bench and supplied with treated
459 urban wastewater.

460 Based on OCT results, the thickness and the volume of the biofouling were higher in
461 the inlet of the channel (mostly in the first baffle) in all the drippers and close to the return
462 areas of the labyrinths in 1 and 2 l.h⁻¹ drippers. The biofouling at the inlet of the dripper
463 increased over time in all three dripper types (1, 2 and 4 l.h⁻¹) tested here but the 1 l.h⁻¹
464 dripper type was more sensitive. Previous studies had found that clogging capacity is more
465 influenced by the geometrie of the dripper channel than flow rate (G. Y. Li et al., 2006; Li et
466 al., 2019). In this study, as Lavanholi et al., (2018) and Li et al., (2019), the dripper flow path
467 with smaller cross-section and average cross-section velocity (v), W/D or $D_h^{1/2}/L$ parameters
468 were relatively weaker in the anti-clogging risk. Dripper flow path with larger v would locally
469 induce a greater turbulence. Thus, the greater near-wall shear stress would accelerate the
470 detachment of biofouling, which would facilitate the removal of the biofouling (Ait-Mouheb
471 et al., 2018; Al-Muhammad et al., 2019). Previous numerical studies have shown that the
472 greatest head loss occurs in the first inlet baffles (Al-Muhammad et al., 2019, 2016) and that
473 the water velocities and turbulent kinetic energy is characterized by low values in corners of
474 dripper channel (Al-Muhammad et al., 2016). Thus, the reduction of velocity in inlet channel
475 can enhance the adhesion and deposition on the wall surface (Ait-Mouheb et al., 2018),

476 explaining the sensitivity to fouling of these areas. In addition, using OCT we observed the
477 biofouling level from the 1 and 2 l.h⁻¹ drippers tended to decreased after the inlet areas as
478 observed by Ait-Mouheb et al., (2018) but re-increased close to the return areas. The return
479 areas was present in the 1 and 2 l.h⁻¹ drippers only and seemed to be sensitive to fouling. One
480 explanation to explain the biofouling close to the return area is that the large bend modifies
481 abruptly the flow behaviour which becomes similar to the inlet area. Studies on biofilm from
482 straight pipe shown that these differences can influenced the mass transfert (nutrients) and so
483 the biofilm development (Araújo et al., 2016). Then, CFD studies would be performed to link
484 the biofouling accumulation and local hydrodynamic conditions.

485 In the present study, biofouling was monitored by OCT in each baffle of the inlet
486 channel. The dripper biofouling alternated between up and down phases locally, mainly for
487 the 1 l.h⁻¹ dripper type with smaller cross-section and low flow rate. This suggests that
488 monitoring the development of local biofouling should be considered to optimize control
489 methods. The down phases may be linked with detachment events (Flemming and Wingender,
490 2010). Detachment events appeared to occur more frequently in the 1 l.h⁻¹ drippers. Several
491 studies have shown that there is a link between biofilm development, production of
492 extracellular polymeric substances (EPS) and hydrodynamic conditions. EPS are essential to
493 ensure the maintenance and stability of the biofilm on a surface. Biofilms grown under low
494 velocities are subject to lower shear stress forces which favour faster growth (Melo and
495 Vieira, 1999). However, biofilms subjected to low flow constraints have limited mechanical
496 strength and are more prone to sloughing than those formed at higher flows (Teodósio et al.,
497 2011). In this study, EPS characterisation and quantification were not performed due to low
498 biofilm quantity inside a dripper. However, even if the hydrodynamic forces associated to the
499 dripper types drive the bacterial composition of the biofilm, the response could also be in the
500 modification of the structure and composition of the biofilm matrix. Further research using

501 OCT combined with EPS characterisation methods and with microbial composition analysis
502 will advance our understanding of biofouling in drippers.

503 The structure of bacterial community of the RWW has a direct influence on the
504 structure and composition of the dripper biofilms. Members of the Comamonadaceae family
505 (β -Proteobacteria including *Hydrogenophaga* genus) dominated in the biofilm samples taken
506 at 32 and 72 days, but were replaced by the Bacteroidetes_VadinHA17 wastewater sludge
507 group belonging to Bacteroidetes at the end (Table S3). This gram-negative, non-mobile
508 anaerobic group is often found in sewage treatment plant sludge and indicates that over time,
509 bacteria commonly found in wastewater have become established and have become the
510 majority in communities. The Comamonadaceae family, which includes many denitrifier
511 members, has been found in wastewater treatment plants and was involved in the first phases
512 of fouling of membrane bioreactors fed with wastewater (Ziegler et al., 2016). Other phyla
513 such as Spirochaetae and Chlorobi appeared in the RWW over time and eventually in the
514 biofilms (Figure 4). The RWW used in this study was obtained after treatment by lagooning
515 and the treatment process can affect the structure and bacterial composition of biofilms.
516 Further research are needed to study the effect of the wastewater treatment processes on
517 biofilm composition in irrigation lines in order to improve management of biofilm
518 development in the drippers.

519 DNA concentration increased over time in the dripper biofilms whereas the bacterial
520 concentration remained stable. This could be explained by the presence of other types of
521 organisms as algae and eukaryotes. Moreover, bacterial predators can influence the structure
522 and composition of the biofilm (Böhme et al., 2009; Parry et al., 2007). As perspective, a
523 metagenomic approach of the function of microorganisms involved in the biofilm formation
524 and the effect of other microorganisms (algae, predators) can complete the understanding of
525 dripper clogging.

526 Bacterial diversity and richness were not influenced by hydraulic parameters of the
527 drippers. This is not consistent with Rochex et al., (2008) who shown that increased shear
528 stress (from 0.055 to 0.27 Pa), corresponding to an increase of the Reynolds number, reduced
529 the bacterial diversity in a Conical Couette–Taylor Reactor. Then differences between the
530 drippers in terms of flow behaviour may not be sufficient to observe an effect on these
531 indices. Although bacterial diversity was not influenced by the hydraulic parameters, the
532 structure of the bacterial community was. These changes are in agreement with the results of
533 previous studies performed on pipe and reactors (Ai et al., 2016; He et al., 2019; Saur et al.,
534 2017). The level of biofouling decreased with an increase of the cross-section velocity (0.34,
535 0.61 and 0.78 m.s⁻¹ for 1, 2 and 4 l.h⁻¹ drippers respectively) in the channel. However the
536 structure of bacterial communities appeared to be less affected by the cross-section velocity
537 above 0.61 m.s⁻¹ (2 l.h⁻¹ dripper). Even though previous studies have shown that the increase
538 in velocity and shear forces influence the spatial organization and structure of the bacterial
539 community (Saur et al., 2017), the differences between the 2 and 4 l.h⁻¹ drippers may not be
540 sufficient to influence this community in the first phases of biofilm development. This could
541 explain similarities in the structure of the bacterial communities sampled in 2 and 4 l.h⁻¹
542 drippers compared to the 1 l.h⁻¹ dripper biofilms until 115 days, and this in spite of the flow
543 differences due to the geometry of the labyrinths (e.g. return zone).

544 Proteobacteria, Bacteroidetes, Firmicutes and Chloroflexi were the most abundant
545 phyla in all three types of dripper (Figure 4). These phyla have been already been described in
546 drippers supplied by treated wastewater (Lequette et al., 2019; Song et al., 2019; Zhou et al.,
547 2013). Over time, the relative abundance of Proteobacteria and more specifically β -
548 Proteobacteria decreased significantly in 1 l.h⁻¹ dripper biofilms compared to 2 and 4 l.h⁻¹
549 dripper biofilms. β -Proteobacteria have been reported to be a dominant group in both drinking
550 water biofilms (Douterelo et al., 2013) and wastewater biofilms (Biswas and Turner, 2012;

551 Ma et al., 2013) and could play an important role in the formation of biofilm in drippers. This
552 group can easily attach to surfaces and can withstand high water velocity and high shear force
553 (Douterelo et al., 2013), which may explain their dominance in drippers 2 and 4 l.h⁻¹.

554 Chloroflexi and Bacteroidetes phyla were also abundant in dripper biofilms.
555 Anaerolineaceae family members (Chloroflexi) were more abundant in 1 l.h⁻¹ dripper biofilms
556 at the end than in 2 and 4 l.h⁻¹ dripper, meaning that Chloroflexi are sensible to the high
557 Reynolds number. These phyla are commonly found in activated sludge of wastewater
558 treatment plants and include filamentous bacteria as Anaerolineaceae family members
559 (Chloroflexi). Research has shown that filamentous bacteria are essential to the formation of
560 activated sludge but when they are over-concentrated, they are responsible for foaming and
561 bulking events (Kragelund et al., 2008, 2007; Nielsen et al., 2009) and for fouling membrane
562 bioreactors in wastewater treatment plants (Li et al., 2008; Rehman et al., 2020). But the
563 increase of Anaerolineaceae over time can also be explained by the interaction with other
564 bacteria. Chloroflexi and *Hydrogenophaga* spp (Proteobacteria phylum), mainly found in 1
565 l.h⁻¹ drippers, were also observed by Ziegler et al. (2016) who studied the biofouling of a
566 pilot-scale membrane bioreactor fed with wastewater. From a physiological point of view,
567 *Hydrogenophaga* spp. are able to synthesise polymeric substances (Calderer et al., 2014).
568 Filamentous Chloroflexi produce a complex of enzymes able to degrade EPS, in turn,
569 enabling the cells to use EPS as substrate to maintain their activities (Kragelund et al., 2007).
570 EPS produced by *Hydrogenophaga* spp could facilitate fouling due to filamentous bacteria
571 and flow parameters. Thus, the increase in Chloroflexi abundance over time could be
572 explained by a sufficient EPS synthesis rate and by the presence of *Hydrogenophaga* spp at
573 the early stage of biofilm formation. Thus, further research on the role of filamentous bacteria
574 in biofouling development is required, especially by focusing on the effect of the hydraulic
575 and geometric parameters of the flow path on their abundancy.

576 The divergence between the 1 l.h⁻¹ drippers and the 2 and 4 l.h⁻¹ drippers prevailed
577 over time and was mainly driven by *Hydrogenophaga* and *Pseudoxanthomonas* genera
578 (Figure 5). Although no clear information is available on the effect of hydraulic conditions on
579 the installation of these two bacterial genera in drippers, they are often found in biofilms
580 associated with membrane reactor fouling supplied by wastewater (Zheng et al., 2018; Ziegler
581 et al., 2016). Contrary to the 1 l.h⁻¹ dripper biofilms, biofilms from the 4 l.h⁻¹ dripper were
582 mainly driven by *Aquabacterium* (Proteobacteria) and *Ideonella* (Proteobacteria,
583 Comamonadaceae family) genera after 4 months. These genera were already found associated
584 to wastewater biofilms (Lequette et al., 2019; Luo et al., 2017; McCormick et al., 2016) and
585 included species able to metabolize plasticizers used in plastics (Kalmbach et al., 1999;
586 Tanasupawat et al., 2016). Thus the type of material and the hydraulic parameters of the
587 drippers could influence the presence of bacteria with specific metabolic activities over time.

588 5. Conclusion

589 The combined use of OCT and high throughput sequencing highlighted the influence of
590 hydrodynamic parameters (flow rate, cross-section) of the drippers supplied with RWW on
591 biofilm development and bacterial communities:

- 592 1) Biofouling was facilitated close to the inlet and in the vortex zones of the dripper
593 channels, more specifically in 1 l.h⁻¹ drippers where the Reynolds number, cross-
594 section and average cross-section velocity (v), W/D or $D_h^{1/2}/L$ were smaller.
- 595 2) The dripper geometry influence the hydraulic flow behaviour (inlet Reynold
596 number and average cross-section velocity) and the structure of bacterial
597 communities in biofilms. However, the structure of the bacterial community from
598 the 2 and 4 l.h⁻¹ drippers were more similar than the 1 l.h⁻¹ dripper biofilms.
- 599 3) The relative abundance of filamentous bacteria belonging to Chloroflexi phylum
600 was lower in 1 l.h⁻¹ compared to 2 and 4 l.h⁻¹.

601 Water velocity evolves along the channel with low velocities at the inlet and in the vortex
602 zones. These changes can influence the transport of nutrients to the biofilm along the channel.
603 Further studies on nutrient transport and on the structure of the bacterial community of the
604 biofilms along the drippers should increase our understanding of fouling phenomena in
605 sensitive areas. Another point is that biofouling can include physical and chemical processes.
606 In this study, the physico-chemical composition of the biofouling was not analysed. Exploring
607 the link between the different types of clogging (physical, chemical and biological) in
608 different dripper types is an important future research path

609 **Acknowledgements**

610 The authors gratefully acknowledge the financial support of the French Water Agency, project
611 “Experimental platform for the reuse of reclaimed wastewater in irrigation, Murviel-lès-
612 Montpellier”. We thank Guillaume Guizard (LBE-INRAE, Narbonne, France) and Jean-
613 François Bonicel (UMR G-Eau-INRAE, Montpellier, France) for their contribution to the
614 development of the dripper system, Geoffrey Froment (UMR G-Eau-INRAE, Montpellier,
615 France), François Liron (UMR G-Eau-INRAE, Montpellier, France) and Marine Muffat-
616 Jeandet (UMR G-Eau-INRAE, Montpellier, France) for their contribution to the development
617 of the test bench, Annabelle Mange (UMR G-Eau-INRAE, Montpellier, France) and Valérie
618 Bru-Adam (LBE-INRAE, Narbonne, France) for their assistance in the field and at laboratory.

619 **Disclosure statement**

620 No potential conflict of interest was reported by the authors. Authors have approved the final
621 article.

622 **References**

623 Ai, H., Xu, J., Huang, W., He, Q., Wang, Y., Ni, B., 2016. Mechanism and kinetics of biofilm
624 growth process influenced by shear stress in sewers. *Water Sci. Technol.* 73, 1572–1582.

625 <https://doi.org/10.2166/wst.2015.633>

626 Ait-Mouheb, N., Schillings, J., Al-Muhammad, J., Bendoula, R., Tomas, S., Amielh, M.,
627 Anselmet, F., 2018. Impact of hydrodynamics on clay particle deposition and biofilm
628 development in a labyrinth-channel dripper. *Irrig. Sci.* 0, 0.
629 <https://doi.org/10.1007/s00271-018-0595-7>

630 Al-Muhammad, J., Tomas, S., Ait-Mouheb, N., Amielh, M., Anselmet, F., 2019.
631 Experimental and numerical characterization of the vortex zones along a labyrinth milli-
632 channel used in drip irrigation. *Int. J. Heat Fluid Flow* 80, 108500.
633 <https://doi.org/10.1016/j.ijheatfluidflow.2019.108500>

634 Al-Muhammad, J., Tomas, S., Anselmet, F., 2016. Modeling a weak turbulent flow in a
635 narrow and wavy channel: case of micro-irrigation. *Irrig. Sci.* 34, 361–377.
636 <https://doi.org/10.1007/s00271-016-0508-6>

637 Araújo, P.A., Malheiro, J., Machado, I., Mergulhão, F., Melo, L., Simões, M., 2016. Influence
638 of Flow Velocity on the Characteristics of *Pseudomonas fluorescens* Biofilms. *J.*
639 *Environ. Eng.* 142, 04016031. [https://doi.org/10.1061/\(ASCE\)EE.1943-7870.0001068](https://doi.org/10.1061/(ASCE)EE.1943-7870.0001068)

640 Besemer, K., 2015. Biodiversity, community structure and function of biofilms in stream
641 ecosystems. *Res. Microbiol.* 166, 774–781. <https://doi.org/10.1016/j.resmic.2015.05.006>

642 Biswas, K., Turner, S.J., 2012. Microbial community composition and dynamics of moving
643 bed biofilm reactor systems treating municipal sewage. *Appl. Environ. Microbiol.* 78,
644 855–864. <https://doi.org/10.1128/AEM.06570-11>

645 Böhme, A., Risse-Buhl, U., Küsel, K., 2009. Protists with different feeding modes change
646 biofilm morphology. *FEMS Microbiol. Ecol.* 69, 158–169.
647 <https://doi.org/10.1111/j.1574-6941.2009.00710.x>

648 Calderer, M., Martí, V., de Pablo, J., Guivernau, M., Prenafeta-Boldú, F.X., Viñas, M., 2014.
649 Effects of enhanced denitrification on hydrodynamics and microbial community
650 structure in a soil column system. *Chemosphere* 111, 112–119.
651 <https://doi.org/10.1016/j.chemosphere.2014.03.033>

652 Clarke, K.R., 1993. Non-parametric multivariate analyses of changes in community structure.
653 *Aust. J. Ecol.* 18, 117–143. <https://doi.org/10.1071/WR9840181>

654 Derlon, N., Peter-Varbanets, M., Scheidegger, A., Pronk, W., Morgenroth, E., 2012.
655 Predation influences the structure of biofilm developed on ultrafiltration membranes.
656 *Water Res.* 46, 3323–3333. <https://doi.org/10.1016/j.watres.2012.03.031>

657 Dosoretz, C.G., Tarchitzky, J., Katz, I., Kenig, E., Chen, Y., 2010. Fouling in Microirrigation
658 Systems Applying Treated Wastewater Effluents. *Treat. Wastewater Agric. Use Impacts*
659 *Soil Environ. Crop.* 328–350. <https://doi.org/10.1002/9781444328561.ch10>

660 Douterelo, I., Sharpe, R.L., Boxall, J.B., 2013. Influence of hydraulic regimes on bacterial
661 community structure and composition in an experimental drinking water distribution
662 system. *Water Res.* 47, 503–516. <https://doi.org/10.1016/j.watres.2012.09.053>

663 Dreszer, C., Wexler, A.D., Drusová, S., Overdijk, T., Zwijnenburg, A., Flemming, H.C.,
664 Kruithof, J.C., Vrouwenvelder, J.S., 2014. In-situ biofilm characterization in membrane
665 systems using Optical Coherence Tomography: Formation, structure, detachment and
666 impact of flux change. *Water Res.* 67, 243–254.
667 <https://doi.org/10.1016/j.watres.2014.09.006>

668 Edgar, R.C., Haas, B.J., Clemente, J.C., Quince, C., Knight, R., 2011. UCHIME improves
669 sensitivity and speed of chimera detection. *Bioinformatics* 27, 2194–2200.
670 <https://doi.org/10.1093/bioinformatics/btr381>

671 Flemming, H., Wingender, J., 2010. The biofilm matrix. *Nat. Rev. Microbiol.* 8, 623–33.
672 <https://doi.org/10.1038/nrmicro2415>

673 G. Y. Li, J. D. Wang, M. Alam, Y. F. Zhao, 2006. Influence of Geometrical Parameters of
674 Labyrinth Path of Drip Emitters on Hydraulic and Anti-clogging Performance. *Trans.*
675 *ASABE* 49, 637–643. <https://doi.org/10.13031/2013.20483>

676 Gamri, S., Soric, A., Tomas, S., Molle, B., Roche, N., 2014. Biofilm development in micro-
677 irrigation emitters for wastewater reuse. *Irrig. Sci.* 32, 77–85.
678 <https://doi.org/10.1007/s00271-013-0414-0>

679 He, Q., Chen, L., Zhang, S., Chen, R., Wang, H., 2019. Hydrodynamic shear force shaped the
680 microbial community and function in the aerobic granular sequencing batch reactors for
681 low carbon to nitrogen (C/N) municipal wastewater treatment. *Bioresour. Technol.* 271,
682 48–58. <https://doi.org/10.1016/j.biortech.2018.09.102>

683 Hou, P., Wang, T., Zhou, B., Song, P., Zeng, W., Li, Y., 2020. Variations in the microbial
684 community of biofilms under different near-wall hydraulic shear stresses in agricultural
685 irrigation systems. *Biofouling* 0, 1–12. <https://doi.org/10.1080/08927014.2020.1714600>

686 Jjemba, P.K., Weinrich, L.A., Cheng, W., Giraldo, E., LeChevallier, M.W., 2010. Regrowth
687 of potential opportunistic pathogens and algae in reclaimed-water distribution systems.
688 *Appl. Environ. Microbiol.* 76, 4169–4178. <https://doi.org/10.1128/AEM.03147-09>

689 Kalmbach, S., Manz, W., Wecke, J., Szewzyk, U., 1999. *Aquabacterium* gen. nov., with
690 description of *Aquabacterium citratiphilum* sp. nov., *Aquabacterium parvum* sp. nov.
691 and *Aquabacterium commune* sp. nov., three in situ dominant bacterial species from the
692 Berlin drinking water system. *Int. J. Syst. Bacteriol.* 49, 769–777.
693 <https://doi.org/10.1099/00207713-49-2-769>

694 Katz, S., Dosoretz, C., Chen, Y., Tarchitzky, J., 2014. Fouling formation and chemical control
695 in drip irrigation systems using treated wastewater. *Irrig. Sci.* 32, 459–469.
696 <https://doi.org/10.1007/s00271-014-0442-4>

697 Kragelund, C., Levantesi, C., Borger, A., Thelen, K., Eikelboom, D., Tandoi, V., Kong, Y.,
698 Krooneman, J., Larsen, P., Thomsen, T.R., Nielsen, P.H., 2008. Identity, abundance and
699 ecophysiology of filamentous bacteria belonging to the Bacteroidetes present in activated
700 sludge plants. *Microbiology* 154, 886–894. <https://doi.org/10.1099/mic.0.2007/011684-0>

701 Kragelund, C., Levantesi, C., Borger, A., Thelen, K., Eikelboom, D., Tandoi, V., Kong, Y.,
702 Van Der Waarde, J., Krooneman, J., Rossetti, S., Thomsen, T.R., Nielsen, P.H., 2007.
703 Identity, abundance and ecophysiology of filamentous Chloroflexi species present in
704 activated sludge treatment plants. *FEMS Microbiol. Ecol.* 59, 671–682.
705 <https://doi.org/10.1111/j.1574-6941.2006.00251.x>

706 Lamm, F.R., Ayars, J.E., Nakayama, F.S., 2007. Maintenance, in: Lamm, F.R., Ayars, J.E.,
707 Nakayama, F.S. (Eds.), *Microirrigation for Crop Production: Design, Operation, and*
708 *Management*, 13th Edn. Elsevier B.V., Amsterdam, pp. 1–643.

709 Lavanholi, R., Oliveira, F.C., Camargo, A.P. de, Frizzone, J.A., Molle, B., Ait-Mouheeb, N.,
710 Tomas, S., 2018. Methodology to Evaluate Dripper Sensitivity to Clogging due to Solid
711 Particles: An Assessment. *Sci. World J.* 2018, 1–9.
712 <https://doi.org/10.1155/2018/7697458>

713 Lazarova, V., Bahri, A., 2005. *Water Reuse for Irrigation*. CRC Press;, Boca Raton.

714 Lehtola, M.J., Laxander, M., Miettinen, I.T., Hirvonen, A., Vartiainen, T., Martikainen, P.J.,
715 2006. The effects of changing water flow velocity on the formation of biofilms and water
716 quality in pilot distribution system consisting of copper or polyethylene pipes. *Water*
717 *Res.* 40, 2151–2160. <https://doi.org/10.1016/j.watres.2006.04.010>

718 Lequette, K., Ait-Mouheb, N., Wéry, N., 2019. Drip irrigation biofouling with treated
719 wastewater: bacterial selection revealed by high-throughput sequencing. *Biofouling* 35,
720 217–229. <https://doi.org/10.1080/08927014.2019.1591377>

721 Li, G.B., Li, Y.K., Xu, T.W., Liu, Y.Z., Jin, H., Yang, P.L., Yan, D.Z., Ren, S.M., Tian, Z.F.,
722 2012. Effects of average velocity on the growth and surface topography of biofilms
723 attached to the reclaimed wastewater drip irrigation system laterals. *Irrig. Sci.* 30, 103–
724 113. <https://doi.org/10.1007/s00271-011-0266-4>

725 Li, J., Li, Y., Ohandja, D.G., Yang, F., Wong, F.S., Chua, H.C., 2008. Impact of filamentous
726 bacteria on properties of activated sludge and membrane-fouling rate in a submerged
727 MBR. *Sep. Purif. Technol.* 59, 238–243. <https://doi.org/10.1016/j.seppur.2007.06.011>

728 Li, Y., Feng, J., Xue, S., Muhammad, T., Chen, X., Wu, N., Li, W., Zhou, B., 2019.
729 Formation mechanism for emitter composite-clogging in drip irrigation system. *Irrig.*
730 *Sci.* 37, 169–181. <https://doi.org/10.1007/s00271-018-0612-x>

731 Li, Y., Yang, P., Ren, S., Xu, T., 2006. Hydraulic Characterizations of Tortuous Flow in Path
732 Drip Irrigation Emitter. *J. Hydrodyn.* 18, 449–457. [https://doi.org/10.1016/S1001-](https://doi.org/10.1016/S1001-6058(06)60119-4)
733 [6058\(06\)60119-4](https://doi.org/10.1016/S1001-6058(06)60119-4)

734 Liu, H., Huang, G., 2009. Laboratory experiment on drip emitter clogging with fresh water
735 and treated sewage effluent. *Agric. Water Manag.* 96, 745–756.
736 <https://doi.org/10.1016/j.agwat.2008.10.014>

737 Luo, J., Lv, P., Zhang, J., Fane, A.G., McDougald, D., Rice, S.A., 2017. Succession of
738 biofilm communities responsible for biofouling of membrane bioreactors (MBRs). *PLoS*
739 *One* 12, 1–23. <https://doi.org/10.1371/journal.pone.0179855>

740 Ma, J., Wang, Z., Zou, X., Feng, J., Wu, Z., 2013. Microbial communities in an anaerobic

741 dynamic membrane bioreactor (AnDMBR) for municipal wastewater treatment:
742 Comparison of bulk sludge and cake layer. *Process Biochem.* 48, 510–516.
743 <https://doi.org/10.1016/j.procbio.2013.02.003>

744 Mahfoud, C., El Samrani, A., Mouawad, R., Hleihel, W., El Khatib, R., Lartiges, B.S.,
745 Ouaïni, N., 2009. Disruption of biofilms from sewage pipes under physical and chemical
746 conditioning. *J. Environ. Sci.* 21, 120–126. [https://doi.org/10.1016/S1001-](https://doi.org/10.1016/S1001-0742(09)60021-8)
747 [0742\(09\)60021-8](https://doi.org/10.1016/S1001-0742(09)60021-8)

748 McCormick, A.R., Hoellein, T.J., London, M.G., Hittie, J., Scott, J.W., Kelly, J.J., 2016.
749 Microplastic in surface waters of urban rivers: Concentration, sources, and associated
750 bacterial assemblages. *Ecosphere* 7. <https://doi.org/10.1002/ecs2.1556>

751 McMurdie, P., Holmes, S., 2012. PHYLOSEQ: a bioconductor package for handling and
752 analysis of high-throughput phylogenetic sequence data. *Pac Symp Biocomput* 235–246.

753 Melo, L.F., Vieira, M.J., 1999. Physical stability and biological activity of biofilms under
754 turbulent flow and low substrate concentration. *Bioprocess Eng.* 20, 363–368.
755 <https://doi.org/10.1007/s004490050604>

756 Nguyen, N.-P., Warnow, T., Pop, M., White, B., 2016. A perspective on 16S rRNA
757 operational taxonomic unit clustering using sequence similarity. *npj Biofilms*
758 *Microbiomes* 2, 16004. <https://doi.org/10.1038/npjbiofilms.2016.4>

759 Nielsen, P.H., Kragelund, C., Seviour, R.J., Nielsen, J.L., 2009. Identity and ecophysiology of
760 filamentous bacteria in activated sludge. *FEMS Microbiol. Rev.* 33, 969–998.
761 <https://doi.org/10.1111/j.1574-6976.2009.00186.x>

762 Niu, W., Liu, L., Chen, X., 2013. Influence of fine particle size and concentration on the
763 clogging of labyrinth emitters. *Irrig. Sci.* 31, 545–555. <https://doi.org/10.1007/s00271->

764 012-0328-2

765 Oliveira, F., Lavanholi, R., Camargo, A., Frizzone, A., Ait-Mouheb, N., Tomas, S., Molle, B.,
766 2017. Influence of Concentration and Type of Clay Particles on Dripper Clogging. *Irrig.*
767 *Drain. Syst. Eng.* 06, 1–5. <https://doi.org/10.4172/2168-9768.1000184>

768 Parry, J.D., Holmes, A.K., Unwin, M.E., Laybourn-Parry, J., 2007. The use of ultrasonic
769 imaging to evaluate the effect of protozoan grazing and movement on the topography of
770 bacterial biofilms. *Lett. Appl. Microbiol.* 45, 364–370. [https://doi.org/10.1111/j.1472-](https://doi.org/10.1111/j.1472-765X.2007.02213.x)
771 [765X.2007.02213.x](https://doi.org/10.1111/j.1472-765X.2007.02213.x)

772 Percival, S.L., Knapp, J.S., Wales, D.S., Edyvean, R.G.J., 1999. The effect of turbulent flow
773 and surface roughness on biofilm formation in drinking water. *J. Ind. Microbiol.*
774 *Biotechnol.* 22, 152–159. <https://doi.org/10.1038/sj.jim.2900622>

775 Qian, J., Horn, H., Tarchitzky, J., Chen, Y., Katz, S., Wagner, M., 2017. Water quality and
776 daily temperature cycle affect biofilm formation in drip irrigation devices revealed by
777 optical coherence tomography. *Biofouling* 7014, 1–11.
778 <https://doi.org/10.1080/08927014.2017.1285017>

779 Rehman, Z.U., Fortunato, L., Cheng, T., Leiknes, T.O., 2020. Metagenomic analysis of
780 sludge and early-stage biofilm communities of a submerged membrane bioreactor. *Sci.*
781 *Total Environ.* 701, 134682. <https://doi.org/10.1016/j.scitotenv.2019.134682>

782 Rickard, A.H., Mcbain, A.J., Stead, A.T., Gilbert, P., 2004. Shear Rate Moderates
783 Community Diversity in Freshwater Biofilms Shear Rate Moderates Community
784 Diversity in Freshwater Biofilms. *Society* 70, 7426–7435.
785 <https://doi.org/10.1128/AEM.70.12.7426>

786 Rochex, A., Godon, J.J., Bernet, N., Escudié, R., 2008. Role of shear stress on composition,

787 diversity and dynamics of biofilm bacterial communities. *Water Res.* 42, 4915–4922.
788 <https://doi.org/10.1016/j.watres.2008.09.015>

789 Saur, T., Morin, E., Habouzit, F., Bernet, N., Escudié, R., 2017. Impact of wall shear stress on
790 initial bacterial adhesion in rotating annular reactor. *PLoS One* 12, 1–19.
791 <https://doi.org/10.1371/journal.pone.0172113>

792 Schindelin, J., Arganda-Carrera, I., Frise, E., Verena, K., Mark, L., Tobias, P., Stephan, P.,
793 Curtis, R., Stephan, S., Benjamin, S., Jean-Yves, T., Daniel, J.W., Volker, H., Kevin, E.,
794 Pavel, T., Albert, C., 2009. Fiji - an Open platform for biological image analysis. *Nat.*
795 *Methods* 9, 241. <https://doi.org/10.1038/nmeth.2019.Fiji>

796 Schloss, P.D., Westcott, S.L., Ryabin, T., Hall, J.R., Hartmann, M., Hollister, E.B.,
797 Lesniewski, R.A., Oakley, B.B., Parks, D.H., Robinson, C.J., Sahl, J.W., Stres, B.,
798 Thallinger, G.G., Van Horn, D.J., Weber, C.F., 2009. Introducing mothur: open-source,
799 platform-independent, community-supported software for describing and comparing
800 microbial communities. *Appl. Environ. Microbiol.* 75, 7537–41.
801 <https://doi.org/10.1128/AEM.01541-09>

802 Song, P., Zhou, B., Feng, G., Brooks, J.P., Zhou, H., Zhao, Z., Liu, Y., Li, Y., 2019. The
803 influence of chlorination timing and concentration on microbial communities in labyrinth
804 channels: implications for biofilm removal. *Biofouling* 1–15.
805 <https://doi.org/10.1080/08927014.2019.1600191>

806 Tanasupawat, S., Takehana, T., Yoshida, S., Hiraga, K., Oda, K., 2016. *Ideonella sakaiensis*
807 sp. nov., isolated from a microbial consortium that degrades poly(ethylene terephthalate).
808 *Int. J. Syst. Evol. Microbiol.* 66, 2813–2818. <https://doi.org/10.1099/ijsem.0.001058>

809 Teodósio, J.S., Simões, M., Melo, L.F., Mergulhão, F.J., 2011. Flow cell hydrodynamics and
810 their effects on *E. coli* biofilm formation under different nutrient conditions and

811 turbulent flow. *Biofouling* 27, 1–11. <https://doi.org/10.1080/08927014.2010.535206>

812 Wagner, M., Taherzadeh, D., Haisch, C., Horn, H., 2010. Investigation of the mesoscale
813 structure and volumetric features of biofilms using optical coherence tomography.
814 *Biotechnol. Bioeng.* 107, 844–853. <https://doi.org/10.1002/bit.22864>

815 Wang, J., Gong, S., Xu, D., Yu, Y., Zhao, Y., 2013. Impact of drip and level-basin irrigation
816 on growth and yield of winter wheat in the North China Plain. *Irrig. Sci.* 31, 1025–1037.
817 <https://doi.org/10.1007/s00271-012-0384-7>

818 Wang, Y., Qian, P.Y., 2009. Conservative fragments in bacterial 16S rRNA genes and primer
819 design for 16S ribosomal DNA amplicons in metagenomic studies. *PLoS One* 4.
820 <https://doi.org/10.1371/journal.pone.0007401>

821 Wei, Z., 2011. Application of RP and Manufacturing to Water-Saving Emitters, in: *Advanced*
822 *Applications of Rapid Prototyping Technology in Modern Engineering.* InTech.
823 <https://doi.org/10.5772/22401>

824 Wei, Z., Cao, M., Liu, X., Tang, Y., Lu, B., 2012. Flow behaviour analysis and experimental
825 investigation for emitter micro-channels. *Chinese J. Mech. Eng. (English Ed.* 25, 729–
826 737. <https://doi.org/10.3901/CJME.2012.04.729>

827 West, S., Wagner, M., Engelke, C., Horn, H., 2016. Optical coherence tomography for the in
828 situ three-dimensional visualization and quantification of feed spacer channel fouling in
829 reverse osmosis membrane modules. *J. Memb. Sci.* 498, 345–352.
830 <https://doi.org/10.1016/j.memsci.2015.09.047>

831 Worako, A.W., 2015. Evaluation of the water quality status of Lake Hawassa by using water
832 quality index , Southern Ethiopia. *Int. J. Water Resour. Environ. Eng.* 7, 58–65.
833 <https://doi.org/10.5897/IJWREE2014>.

834 Xiao, Y., Seo, Y., Lin, Y., Li, L., Muhammad, T., Ma, C., Li, Y., 2020. Electromagnetic
835 fields for biofouling mitigation in reclaimed water distribution systems. *Water Res.* 173,
836 115562. <https://doi.org/10.1016/j.watres.2020.115562>

837 Yan, D., Bai, Z., Rowan, M., Gu, L., Shumei, R., Yang, P., 2009. Biofilm structure and its
838 influence on clogging in drip irrigation emitters distributing reclaimed wastewater. *J.*
839 *Environ. Sci.* 21, 834–841. [https://doi.org/10.1016/S1001-0742\(08\)62349-9](https://doi.org/10.1016/S1001-0742(08)62349-9)

840 Yan, D., Yang, P., Rowan, M., Ren, S., Pitts, D., 2010. Biofilm Accumulation and Structure
841 in the Flow Path of Drip Emitters Using Reclaimed Wastewater. *Trans. Asabe* 53, 751–
842 758. <https://doi.org/10.13031/2013.30080>

843 Yu, Y., Lee, C., Kim, J., Hwang, S., 2005. Group-specific primer and probe sets to detect
844 methanogenic communities using quantitative real-time polymerase chain reaction.
845 *Biotechnol. Bioeng.* 89, 670–679. <https://doi.org/10.1002/bit.20347>

846 Zhang, J., Zhao, W., Tang, Y., Lu, B., 2010. Anti-clogging performance evaluation and
847 parameterized design of emitters with labyrinth channels. *Comput. Electron. Agric.* 74,
848 59–65. <https://doi.org/10.1016/j.compag.2010.06.005>

849 Zhang, J., Zhao, W., Wei, Z., Tang, Y., Lu, B., 2007. Numerical and experimental study on
850 hydraulic performance of emitters with arc labyrinth channels. *Comput. Electron. Agric.*
851 56, 120–129. <https://doi.org/10.1016/j.compag.2007.01.007>

852 Zhang, L., Wu, P., Zhu, D., Zheng, C., 2016. Flow regime and head loss in a drip emitter
853 equipped with a labyrinth channel. *J. Hydrodyn.* 28, 610–616.
854 [https://doi.org/10.1016/S1001-6058\(16\)60665-0](https://doi.org/10.1016/S1001-6058(16)60665-0)

855 Zheng, L., Yu, D., Wang, G., Yue, Z., Zhang, C., Wang, Y., Zhang, J., Wang, J., Liang, G.,
856 Wei, Y., 2018. Characteristics and formation mechanism of membrane fouling in a full-

857 scale RO wastewater reclamation process: Membrane autopsy and fouling
858 characterization. *J. Memb. Sci.* 563, 843–856.
859 <https://doi.org/10.1016/j.memsci.2018.06.043>

860 Zhou, B., Li, Y., Liu, Y., Zhou, Y., Song, P., 2019. Critical controlling threshold of internal
861 water shear force of anti-clogging drip irrigation emitters using reclaimed water. *Irrig.*
862 *Sci.* 0, 0. <https://doi.org/10.1007/s00271-019-00624-8>

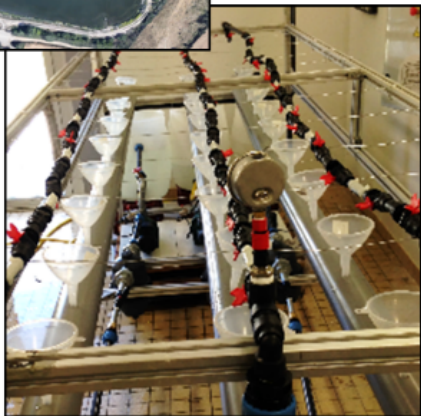
863 Zhou, B., Li, Y., Pei, Y., Liu, Y., Zhang, Z., Jiang, Y., 2013. Quantitative relationship
864 between biofilms components and emitter clogging under reclaimed water drip
865 irrigation. *Irrig. Sci.* 31, 1251–1263. <https://doi.org/10.1007/s00271-013-0402-4>

866 Zhou, B., Wang, T., Li, Y., Bralts, V., 2017. Effects of microbial community variation on bio-
867 clogging in drip irrigation emitters using reclaimed water. *Agric. Water Manag.* 194,
868 139–149. <https://doi.org/10.1016/j.agwat.2017.09.006>

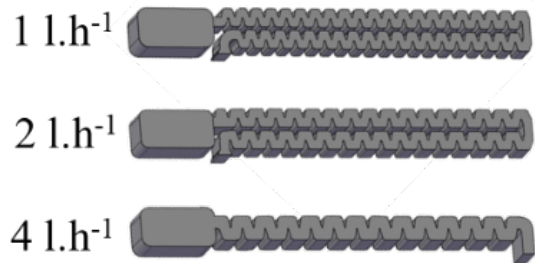
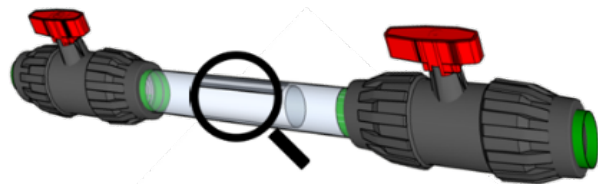
869 Ziegler, A.S., McIlroy, S.J., Larsen, P., Albertsen, M., Hansen, A.A., Heinen, N., Nielsen,
870 P.H., 2016. Dynamics of the fouling layer microbial community in a membrane
871 bioreactor. *PLoS One* 11, 1–14. <https://doi.org/10.1371/journal.pone.0158811>

872

Wastewater treatment plant

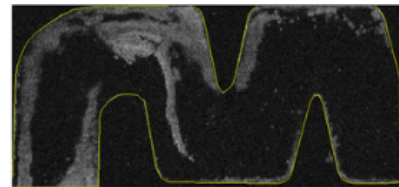


Lab drip irrigation system supplied by reclaimed wastewater



Three irrigation drippers to analyze the effects of flow topology on ...

Biofouling kinetic growth



Microbial composition